

Forecast score distributions with imperfect observations

Julie Bessac,¹ Philippe Naveau²

¹ Mathematics and Computer Science Division, Argonne National Laboratory, Lemont, IL, 60439, USA

² Laboratoire de Sciences du Climat et de l'Environnement, IPSL-CNRS, Gif-sur-Yvette, 91191, France

Abstract

The field of statistics has become one of the mathematical foundations in forecast evaluations studies, especially in regard to computing scoring rules. The classical paradigm of scoring rules is to discriminate between two different forecasts by comparing them with observations. The probability distribution of the observed record is assumed to be perfect as a verification benchmark. In practice, however, observations are almost always tainted by errors and uncertainties. These may be due to homogenization problems, instrumental deficiencies, the need for indirect reconstructions from other sources (e.g., radar data), model errors in gridded products like reanalysis, or any other data-recording issues. If the yardstick used to compare forecasts is imprecise, one can wonder whether such types of errors may or may not have a strong influence on decisions based on classical scoring rules. We propose a new scoring rule scheme in the context of models that incorporate errors of the verification data. We rely on existing scoring rules and incorporate uncertainty and error of the verification data through a hidden variable and the conditional expectation of scores when they are viewed as a random variable. The proposed scoring framework is compared to scores used in practice, and is expressed in various setups, mainly an additive Gaussian noise model and a multiplicative Gamma noise model. By considering scores as random variables one can access the entire range of their distribution. In particular we illustrate that the commonly used mean score can be a misleading representative of the distribution when this latter is highly skewed or have heavy tails. In a simulation study, through the power of a statistical test and the computation of Wasserstein distances between scores distributions, we demonstrate the ability of the newly proposed score to better discriminate between forecasts when verification data are subject to uncertainty compared with the scores used in practice. Finally, we illustrate the benefit of accounting for the uncertainty of the verification data into the scoring procedure on a dataset of surface wind speed from measurements and numerical model outputs.

1 Introduction

Probabilistic forecast evaluation generally involves the comparison of a probabilistic forecast cumulative distribution function (cdf) F (in the following, we assume that F admits a probability density function f) with verification data y that could be of diverse origins (Jolliffe and Stephenson, 2004; Gneiting et al., 2007). In this context verification data are most of the time, but not exclusively, observational data. Questions related to the quality and variability of observational data have been raised and tackled in different scientific contexts. For instance, data assimilation requires careful estimation of uncertainties related

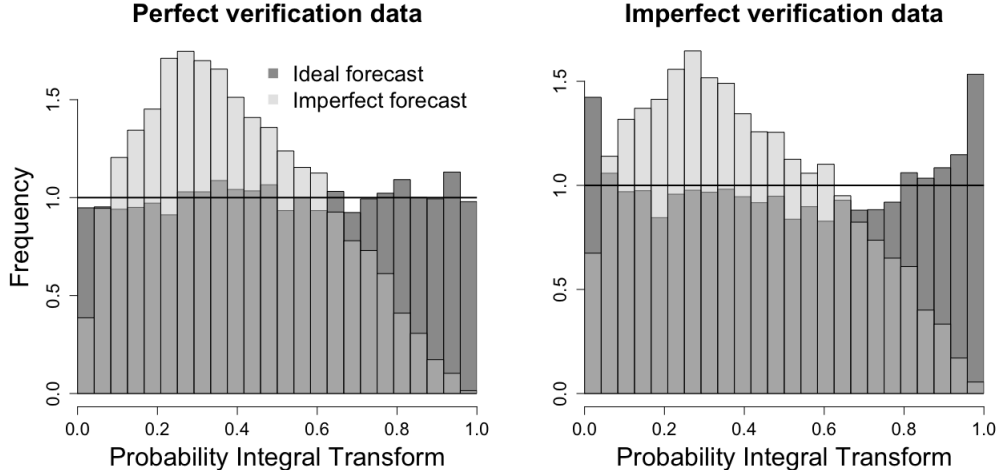


Figure 1: An “ideal” (dark grey) and “imperfect” (light grey) synthetic forecasts, with respective distributions $\mathcal{N}(0, 4)$ and $\mathcal{N}(1, 3)$, are compared with “ideal” verification data (left) with distribution $\mathcal{N}(0, 4)$ and imperfect verification data Y (right) with distribution $\mathcal{N}(0, 3)$. Comparing an ideal forecast to corrupted verification data leads to an apparent under-dispersion of the ideal forecast.

to both numerical models and observations (Daley, 1993; Waller et al., 2014; Janjić et al., 2017). Apart from a few studies (see, e.g. Hamill and Juras, 2006; Ferro, 2017), error and uncertainty associated with the verification data have rarely been addressed in forecast evaluation. Nonetheless, errors in verification data can lead to severe mis-characterization of probabilistic forecasts as illustrated in Figure 1, where an ideal forecast (forecast having the same distribution as the true data) appears under-dispersed when the verification data have a larger variance than the true process. Forecast evaluation can be performed qualitatively through visual inspection of statistics of the data such as in Figure 1 (see, e.g. Bröcker and Ben Bouallègue, 2020), and quantitatively through the use of scalar functions called scores (Gneiting et al., 2007; Gneiting and Raftery, 2007). In this work, we focus on the latter, we illustrate and propose a framework based on hidden variables to embed imperfect verification data into scoring functions.

Motivating example

To illustrate the proposed work, we consider surface wind data from a previous work (Bessac et al., 2018). Time series of ground measurements from the NOAA Automated Surface Observing System (ASOS) network are available at <ftp://ftp.ncdc.noaa.gov/pub/data/asos-onemin> and outputs from numerical weather prediction (NWP) forecasts are generated by using WRF v3.6 (Skamarock et al., 2008), a state-of-the-art numerical weather prediction system designed to serve both operational forecasting and atmospheric research needs. As observed in Figure 2, the uncertainty associated with observation data can affect the evaluation of the forecast. As an extension, if two forecasts were to fall within the uncertainty range of the observations, it would require a non-trivial choice from the forecaster to rank forecasts. We will apply our proposed scoring framework to this dataset in Section 5.3 and compute scores embedding this uncertainty.

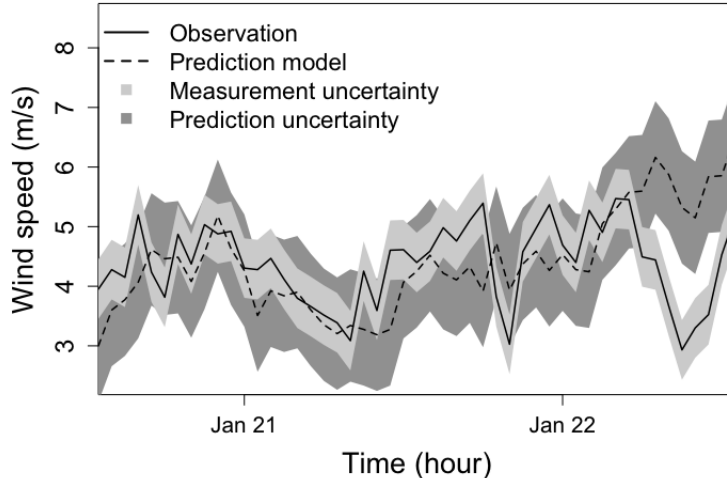


Figure 2: Time series of surface wind speed measurements of two days of January 2012. The solid line represents ground measurements and the light gray shaded area represents observational uncertainty ($\pm\sigma$ with $\sigma = 0.5$ defined in Pinson and Hagedorn (2012)). The dashed line represents a numerical model output and the model uncertainty in dark gray shade.

Imperfect verification data and underlying physical state

In verification and recalibration of ensemble forecasts, an essential verification step is to find data that precisely identify the forecast events of interest, the so-called verification dataset (see, e.g., Jolliffe and Stephenson, 2004). Jolliffe and Stephenson (2004), in Section 1.3 of their book, discussed the uncertainty associated with verification data such as sampling uncertainty, direct measurement uncertainty, or changes in locations in the verification dataset. Verification data arise from various sources and consequently present various types of errors and uncertainties such as measurement error (Dirkson et al., 2019), design and quality: e.g., gridded data versus weather stations, homogeneization problems, sub-sampling variability (Mittermaier and Stephenson, 2015), or mis-matching resolutions as weather or regional as climate models are running at ever finer resolution and increased fidelity with rarely observational data available to evaluate at such scales requiring to account for up- or down-sampling error. In order to provide accurate forecast evaluations, it is crucial to distinguish and account for these types of errors. For instance, the effect of observational error can be stronger at short-term horizon when forecast error is weaker. Additive models have been used for the observational error (Ciach and Krajewski, 1999; Saetra et al., 2004) or used to enhance coarser resolutions to allow comparison with fine resolution data (Mittermaier and Stephenson, 2015). In the following, we will present an additive and a multiplicative framework based on a hidden variable to embed uncertainty in data sources.

A common way of modeling errors is by representing the truth as a hidden underlying process also called state (Kalman, 1960; Kalman and Bucy, 1961). Subsequently each source of data is seen as a proxy of the hidden state and modeled as a function of it. This forms the basis of data assimilation models where the desired state of the atmosphere is estimated through the knowledge of physics-based models and observational data that are both seen as versions of the non-observed true physical state. In the following, we base our scoring

framework on the decomposition of the verification data as a function of a hidden true state, referred to X , and an error term.

Related literature

Uncertainty and errors arise from various sources such as the forecast and-or the verification data (predictability quality, uncertainty, errors, dependence and correlation, time-varying distribution) and the computational approximation of scores. A distribution-based verification approach was initially proposed by Murphy and Winkler (1987), where joint distributions for forecast and observation account for the information and interaction of both datasets. Wilks (2010) studied the effect of serial correlation of forecasts and observations on the sampling distributions of Brier score and in particular serially correlated forecasts inflate its variance. Bolin and Wallin (2019) discussed the misleading use of average scores, in particular for the continuous ranked probability score (CRPS) that is shown to be scale-dependent, when forecasts have varying predictability such as in non-stationary cases or exhibit outliers. More specifically, robustness and scale-invariance corrections of the CRPS are proposed to account for outliers and varying predictability in scoring schemes. Concerning the impact of the forecast density approximation from finite ensembles, Zamo and Naveau (2018) compared four CRPS estimators and highlighted recommendations in terms of the type of ensemble, whether random or a set of quantiles. In addition, several works focus on embedding verification data errors and uncertainties into scoring setups. Some methods aimed at correcting the verification data and use regular scoring metrics, such as perturbed ensemble methods (Anderson, 1996; Hamill, 2001; Bowler, 2008; Gorgas and Dorninger, 2012). Other works modeled observations as random variables and expressed scoring metrics in that context (Candille and Talagrand, 2008; Pappenberger et al., 2009; Pinson and Hagedorn, 2012). Some approaches directly modified the expression of metrics, (Hamill and Juras, 2006; Ferro, 2017), and others (see, e.g. Hamill and Juras, 2006) accounted for varying climatology by sub-dividing the sample into stationary ones. In Ciach and Krajewski (1999) and Saetra et al. (2004), additive errors were embedded in scores via convolution. Analogously to the Brier score decomposition of Murphy (1973), Weijs and Van De Giesen (2011); Weijs et al. (2010) decomposed the Kullback-Leibler divergence score and the cross-entropy score into uncertainty into reliability and resolution components in order to account for uncertain verification data. Kleen (2019) discussed scores scale sensitivity to additive measurement errors and proposed a measure of discrepancy between scores computed on uncorrupted and corrupted verification data.

Proposed scoring framework

The following paper proposes an idealized framework to express commonly used scores with observational uncertainty and errors. The new framework relies on the decomposition of the verification data into a “true” hidden state and an error term, and on the representation of scores as a random variable when the verification data is seen as a random variable. Section 2 introduces a scoring framework that accounts for errors in the verification data for scores used in practice. Sections 3 and 4 respectively implement the additive and multiplicative error-embedding cases for the proper logarithmic score (log-score) and proper CRPS. Section 5 illustrates the merits of scores in a simulation context and a in real application case. Finally, Section 6 provides a final discussions and insights in future works.

2 Scoring rules under uncertainty

In the following, we propose a version of scores based on the conditional expectation of what is defined an “ideal” score given the verification data tainted by errors, when scores are viewed as random variables. The idea of conditional expectation was also used in Ferro (2017), but with a different conditioning.

2.1 Scores as random variables

In order to build the proposed score version as well as to interpret scores further than through their mean and assess for their uncertainty, we will rely on scores represented as random variables. In practice, scores are averaged over all available verification data y , and the uncertainty associated with this averaged score is mostly neglected. However this uncertainty reveals to be significant as pointed it out in Dirkson et al. (2019) where confident intervals were computed through bootstrapping. In order to assess, the probability distribution of score s_0 , we assume Y is a random variable representing the verification data y and write a score as a random variable $s_0(F, Y)$, where F is the forecast cdf to be evaluated. This representation gives access to the score distribution and enables to explore the uncertainty of this latter. A few works in the literature have already considered scores as random variables and performed associated analysis. In Diebold and Mariano (2002) and Jolliffe (2007), scores distributions were considered to build confidence intervals and hypothesis testing to assess differences in scores values when comparing forecasts to the climatology. In Wilks (2010), the effect of serial correlation on the sampling distributions of Brier score was investigated. Pinson and Hagedorn (2012) illustrated and discussed scores distributions across different prediction horizons and across different level of observational noise.

2.2 Hidden state and scoring

Scores used in practice are evaluated on verification data y , $s_0(F, y)$. We define the “ideal” score as $s_0(F, x)$, where x is the realization of the hidden underlying “true” state that gives rise to the verification data y . Ideally, one would use x to provide the best assessment of forecast F quality through $s_0(F, x)$; however since x is not available, we consider the best approximation of $s_0(F, x)$ given the observation y in terms of L^2 -norm via the conditional expectation. In Ferro (2017), the conditional expectation of the observed score was considered given the true state X . For a given score s_0 , we propose the following score version $s_v(., y)$:

$$s_v(F, y) = \mathbb{E}(s_0(F, X)|Y = y) \quad (1)$$

where X is the true hidden state, Y is the random variable representing the available observation used as verification data, and F is the forecast cdf to be evaluated. The following properties hold for the score s_v :

$$\begin{aligned} \mathbb{E}_X[s_0(F, X)] &= \mathbb{E}_Y[s_v(F, Y)] \\ \mathbb{V}_X[s_0(F, X)] &\geq \mathbb{V}_Y[s_v(F, Y)] \text{ for any forecast cdf } F. \end{aligned} \quad (2)$$

Details of the computations are found in the Appendix. The first equality guaranties that any propriety attached to the mean value of s_0 are preserved with s_v . The second inequality arises from the law of total variance and implies a reduced dispersion of the corrected score

compared to the ideal score. This can be explained by the prior knowledge on the verification data that reduces uncertainty in the score. These properties are illustrated with simulated examples and real data in Section 5.

The proposed score reveals desirable mathematical properties of unbiasedness and variance reduction while accounting for the error in the verification data; however it relies on the knowledge of $[X|Y]$, or equivalently of $[Y|X]$ and $[X]$. Nonetheless, as illustrated in Sections 3 and 4, the simplifying key to the score derivation in Eqn. (1) is to use Bayesian conjugacy when applicable. This is illustrated in the following sections with a Gaussian additive case and a Gamma multiplicative case. In Section 5, we illustrate the proposed score derivation in a real application case.

3 Gaussian additive case

As discussed earlier, a commonly used setup in applications is when errors are additive and their natural companion distribution is Gaussian. Hereafter, we derive the score from Eqn. (1) for the commonly used log-score and CRPS in the Gaussian additive case, where the hidden state X and the verification data Y are linked through the following system:

$$\text{Model (A)} \quad \begin{cases} X \sim \mathcal{N}(\mu_0, \sigma_0^2), \\ Y = X + \mathcal{N}(0, \omega^2), \end{cases}$$

where Y is the observed verification data, X is the hidden true state, and all Gaussian variables are assumed independent. In the following, for simplicity we consider $\mathbb{E}(X) = \mathbb{E}(Y)$; however one can update the model easily to a mean-biased verification data Y . Parameters are supposed to be known from the applications, one could use priors on the parameters when estimates are not available. In the following, we express different versions of the proper log-score and CRPS: the ideal version, the used-in-practise version, and the error-embedding version from Eqn. (1).

3.1 Log-score versions

For a Gaussian predictive pdf f with mean μ and variance σ^2 , the proper log-score is defined by

$$s_0(f, x) = \log \sigma + \frac{1}{2\sigma^2}(x - \mu)^2 + \frac{1}{2} \log 2\pi, \quad (3)$$

has been widely used in the literature. Ideally, one would access the true state X and evaluate forecast against its realizations x ; however since X is not accessible scores are computed against observations y :

$$s_0(f, y) = \log \sigma + \frac{1}{2\sigma^2}(y - \mu)^2 + \frac{1}{2} \log 2\pi. \quad (4)$$

Applying basic properties of Gaussian conditioning, our score defined by (1) can be written as:

$$\begin{aligned} s_v(f, y) &= \log \sigma + \frac{1}{2\sigma^2} \left\{ \frac{\omega^2 \sigma_0^2}{\sigma_0^2 + \omega^2} + (\bar{y} - \mu)^2 \right\} + \frac{1}{2} \log 2\pi \\ &\quad \text{with } \bar{y} = \frac{\omega^2}{\sigma_0^2 + \omega^2} \mu_0 + \frac{\sigma_0^2}{\sigma_0^2 + \omega^2} y. \end{aligned} \quad (5)$$

Details of the computations are found in the Appendix.

3.2 CRPS versions

Besides the logarithmic score, the CRPS is another classical proper scoring rule used in weather forecast centers. It is defined as

$$c_0(f, x) = \mathbb{E}|Z - x| - \frac{1}{2}\mathbb{E}|Z - Z'|, \quad (6)$$

where Z and Z' are *i.i.d.* copy random variables with continuous pdf f . The CRPS can be rewritten as $c_0(f, x) = x + 2\mathbb{E}(Z - x)_+ - 2\mathbb{E}(Z\bar{F}(Z))$, where $(Z - x)_+$ represents the positive part of $Z - x$ and $\bar{F}(x) = 1 - F(x)$ corresponds to the survival function associated to the cdf F . For example, the CRPS for a Gaussian forecast with parameters μ and σ is equal to

$$c_0(f, x) = x + 2\sigma \left[\phi\left(\frac{x - \mu}{\sigma}\right) - \frac{x - \mu}{\sigma} \Phi\left(\frac{x - \mu}{\sigma}\right) \right] - \left[\mu + \frac{\sigma}{\sqrt{\pi}} \right], \quad (7)$$

where ϕ and Φ are the pdf and cdf of a standard normal distribution (Gneiting et al., 2005; Taillardat et al., 2016). Similarly to (4), in practice one evaluates (7) against observations y since the hidden state X is unobserved.

Under the Gaussian additive model (A), the proposed CRPS defined by Eqn. (1) is written as

$$c_v(f, \bar{y}) = \bar{y} + 2\sigma_\omega \left[\phi\left(\frac{\bar{y} - \mu}{\sigma_\omega}\right) - \frac{\bar{y} - \mu}{\sigma_\omega} \Phi\left(\frac{\bar{y} - \mu}{\sigma_\omega}\right) \right] - \left[\mu + \frac{\sigma}{\sqrt{\pi}} \right], \quad (8)$$

where $\sigma_\omega^2 = \sigma^2 + \frac{\omega^2\sigma_0^2}{\sigma_0^2 + \omega^2}$ and $\bar{y} = \frac{\omega^2}{\sigma_0^2 + \omega^2}\mu_0 + \frac{\sigma_0^2}{\sigma_0^2 + \omega^2}$. Details of the computations are found in the Appendix.

3.3 Scores distributions

Under the Gaussian additive model (A), the random variables associated with the proposed log-scores defined by (4) and (5) is written as

$$s_0(f, Y) \stackrel{d}{=} a_0 + b_0\chi_0^2, \quad \text{and} \quad s_v(f, Y) \stackrel{d}{=} a_v + b_v\chi_v^2, \quad (9)$$

where $\stackrel{d}{=}$ means equality in distribution and χ_0^2 and χ_v^2 noncentral chi-squared random variables with 1 *d.o.f.* and respective non-centrality parameters λ_0 and λ_v . The explicit expressions of the constants λ_0 , λ_v , a_0 , a_v , b_0 and b_v are found in the Appendix. The distribution of $s_0(f, X)$ can be derived similarly. Figure 3 illustrates the distributions in (9) for various values of the noise parameter ω . The distributions are very peaked due to the single degree of freedom of the Chi-square distribution, moreover their bulks are far from the true mean of the ideal score of $s_0(\cdot, X)$ challenging the use of the mean score to compare forecasts. The concept of propriety is based on averaging scores; however the asymmetry and long right tails of the noncentral chi-squared densities makes the mean a non-reliable statistic to represent such distributions. Bolin and Wallin (2019) discussed the misleading use of averaged scores in the context of time-varying predictability where different scales of prediction errors arise generating different of order of magnitude of evaluated scores. However, the newly proposed scores exhibit a bulk of their distribution closer to the mean and with a reduced variance as stated in Eqn. (2), leading to more confidence in the mean when this latter is consider.

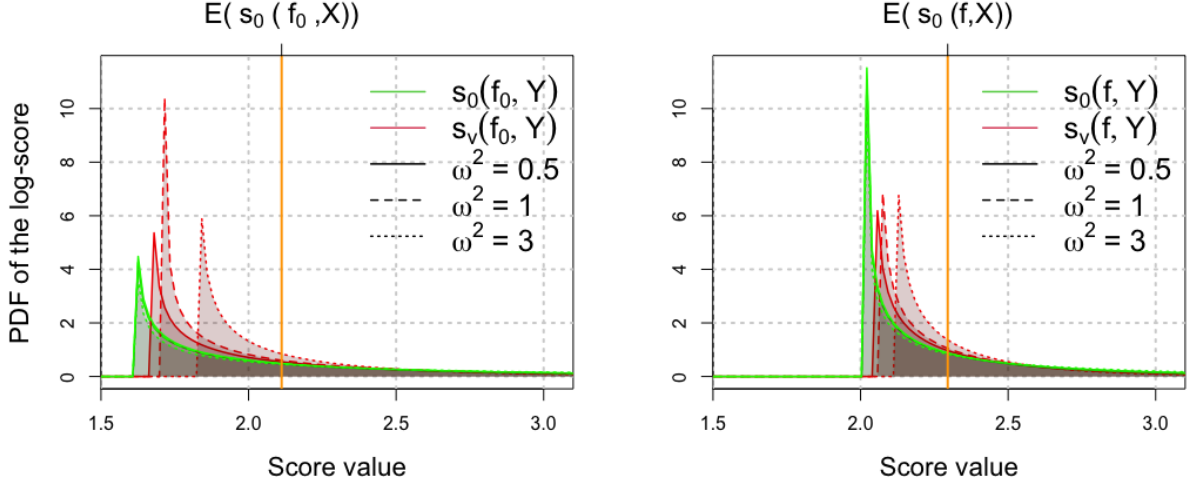


Figure 3: Probability distribution functions (pdf) from Eqn. (9) of the log-score used in practice $s_0(\cdot, Y)$ (green) and the proposed score $s_v(\cdot, Y)$ (red) computed for the ideal forecast f_0 on the left ($\mu = \mu_0 = 0$ and $\sigma = \sigma_0 = 2$) and imperfect forecasts f on the right ($\mu = 1$ and $\sigma = 3$). The mean of the ideal score is depicted with an orange line: $\mathbb{E}(s_0(f_0, X))$ on the left and $\mathbb{E}(s_0(f, X))$ on the right. The following distributions are used: $X \sim \mathcal{N}(0, 4)$ and $Y \sim \mathcal{N}(0, 4 + \omega^2)$ with several levels of observational noise $\omega^2 = 0.5, 1, 3$.

Similarly, under the additive Gaussian model (A), the random variable associated with the proposed CRPS defined by (8) is written as

$$c_v(f, \bar{Y}) = \bar{Y} + 2\sigma_\omega \left[\phi\left(\frac{\bar{Y} - \mu}{\sigma_\omega}\right) - \frac{\bar{Y} - \mu}{\sigma_\omega} \bar{\Phi}\left(\frac{\bar{Y} - \mu}{\sigma_\omega}\right) \right] - \left[\mu + \frac{\sigma}{\sqrt{\pi}} \right], \quad (10)$$

where $\sigma_\omega^2 = \sigma^2 + \frac{\omega^2 \sigma_0^2}{\sigma_0^2 + \omega^2}$ and the random variable $\bar{Y} = \frac{\omega^2}{\sigma_0^2 + \omega^2} \mu_0 + \frac{\sigma_0^2}{\sigma_0^2 + \omega^2} Y$ follows a Gaussian pdf with mean μ_0 and variance $\sigma_0^2 \times \frac{\sigma_0^2}{\sigma_0^2 + \omega^2}$. The distribution of (10) does not belong to any known parametric families; however it is still possible to characterize the score distribution through sampling when the distribution of Y is available. Finally, having access to distributions like (9) or (10) gives access to the whole range of uncertainty of the score distributions helping to derive statistics that are more representative than the mean as pointed out above, and to compute confidence intervals without bootstrapping approximations as in (Wilks, 2010; Dirkson et al., 2019). Finding adequate representatives of a score distribution that shows reliable discriminative skills is beyond the scope of this work. Nevertheless, in Section 5.2 we take forward the concept of score distributions and apply it to computing distances between score distributions in order to assess their discriminative skills.

4 Multiplicative Gamma case

The Gaussian assumption is appropriate when dealing with averages, for example, mean temperatures; however, the normal hypothesis cannot be justified for positive and skewed variables such as precipitation intensities. An often-used alternative in such cases is to use a Gamma distribution, which works fairly well in practice to represent the bulk of rainfall

intensities. Hence, we assume in this section that the true but unobserved X follows a Gamma distribution with parameters α_0 and β_0 : $f_X(x) = \frac{\beta_0^{\alpha_0}}{\Gamma(\alpha_0)} x^{\alpha_0-1} \exp(-\beta_0 x)$, for $x > 0$. For positive random variables such as precipitation, additive models cannot be used to introduce errors. Instead, we prefer to use a multiplicative model of the type

$$\text{Model (B)} \quad \begin{cases} X \sim \text{Gamma}(\alpha_0, \beta_0), \\ Y = X \times \epsilon, \end{cases} \quad (11)$$

where ϵ is a positive random variable independent of X . To make feasible computations, we model the error ϵ as an inverse Gamma pdf with parameters a and b : $f_\epsilon(u) = \frac{b^a}{\Gamma(a)} u^{-a-1} \exp\left(-\frac{b}{u}\right)$, for $u > 0$. The basic conjugate prior properties of such Gamma and inverse Gamma distributions allows us to easily derive the pdf $[X|Y = y]$. Analogously to Section 3, we express the proper log-score and proper CRPS within this multiplicative Gamma model in the following paragraphs.

4.1 Log-score versions

Let us consider a Gamma distribution f with parameters $\alpha > 0$ and $\beta > 0$ for the prediction. With obvious notations, the log-score for this forecast f becomes

$$s_0(f, x) = (1 - \alpha) \log x + \beta x - \alpha \log \beta + \log \Gamma(\alpha). \quad (12)$$

Under the Gamma multiplicative model (B), the random variable associated with the corrected log-scores defined by Eqn. (1) and (12) is expressed as

$$s_v(f, Y) = (1 - \alpha) (\psi(\alpha_0 + a) - \log(\beta_0 + b/Y)) + \beta \frac{\alpha_0 + a}{\beta_0 + b/Y} - \alpha \log \beta + \log \Gamma(\alpha), \quad (13)$$

where $\psi(x)$ represents the digamma function defined as the logarithmic derivative of the Gamma function, namely, $\psi(x) = d \log \Gamma(x) / dx$. Details of the computations are found in the Appendix.

4.2 CRPS versions

For a Gamma forecast with parameters α and β , the corresponding CRPS (see, e.g., Tailard et al., 2016; Scheuerer and Möller, 2015) is equal to

$$c_0(f, x) = \left[\frac{\alpha}{\beta} - \frac{1}{\beta B(.5, \alpha)} \right] - x + 2 \left[\frac{x}{\beta} f(x) + \left(\frac{\alpha}{\beta} - x \right) \bar{F}(x) \right]. \quad (14)$$

Under the multiplicative Gamma model (B), the random variable associated with the CRPS (14) corrected by Eqn. (1) is expressed as

$$\begin{aligned} c_v(f, Y) = & \left[\frac{\alpha}{\beta} - \frac{1}{\beta B(.5, \alpha)} \right] - \frac{\alpha_0 + a}{\beta_0 + \frac{b}{Y}} + 2 \frac{\beta^{\alpha-1} (\beta_0 + b/Y)^{\alpha_0+a}}{B(\alpha, \alpha_0 + a) (\beta + \beta_0 + b/Y)^{\alpha+\alpha_0+a}} \\ & + \frac{2(\beta_0 + b/Y)^{\alpha_0+a}}{\Gamma(\alpha) \Gamma(\alpha_0 + a)} \int_0^{+\infty} \left(\frac{\alpha}{\beta} - x \right) \Gamma(\alpha, \beta x) x^{\alpha_0+a-1} \exp(-(\beta_0 + b/Y)x) dx. \end{aligned} \quad (15)$$

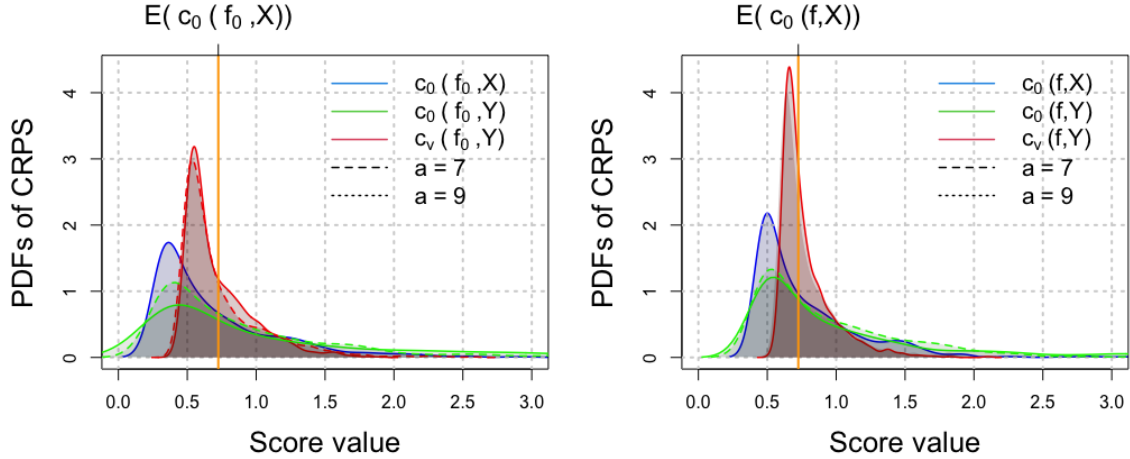


Figure 4: Estimated probability distribution of the CRPS under the multiplicative Gamma model; shown in blue is the distribution of $c_0(., X)$; shown in green is the distribution of $s_0(., Y)$; and shown in red is the distribution of $c_v(., Y)$ respectively from Equations (14) and (15). The mean of the ideal score $\mathbb{E}(c_0(., X))$ is depicted with an orange line. Left: score distributions for the ideal forecast f_0 having the same distribution as X ($\alpha = \alpha_0 = 7$ and $\beta = \beta_0 = 2$) validated against X and corrupted verification data Y with different levels of error: $a = 7, 9$ and $b = 8$. Right: score distributions for the imperfect forecast f with distribution parameters $\alpha = 4$ and $\beta = 1$ validated against X and corrupted verification data Y . The following parameters $\alpha_0 = 7$, $\beta_0 = 2$ are used for the hidden state X .

Details of the computations are found in the Appendix. Similarly to Section 3.3, one can access the range of uncertainty of the proposed scores (13) and (15) when sampling from the distribution of Y is available. As an illustration, Figure 4 shows the distributions of the three CRPS presented in this section. Similarly to the previous section, one can see the benefits of embedding the uncertainty of the verification data are noticeable in the variance reduction of distributions shaded in red and the smaller distance between the bulk of distributions in red and the mean value of the ideal score.

5 Applications and illustrations

The following section applies and illustrates through simulation studies the benefit of accounting for uncertainty in scores as presented in Section 2 through the power analysis of a hypothesis test and the study of Wasserstein distances between score distributions. Finally, we illustrate numerically the motivating example with wind data from Section 1.

5.1 Power analysis of hypothesis testing

In this section, a power analysis of the following hypothesis test is performed on simulated data following Diebold and Mariano (2002) in order to investigate the discriminative skills of the proposed score from Eqn. (1). In Diebold and Mariano (2002), hypothesis tests focused on discriminating forecasts from the climatology; in the current study, we test the ability of the proposed score to discriminate any forecast from the ideal forecast f_0 (forecast having the

“true” hidden state X distribution). Hypothesis tests are tuned to primarily minimize the error of type I (wrongly rejecting the null hypothesis), consequently it is common practice to assess the power of a test. The power p is the probability of rejecting a false null hypothesis, the power expresses as $1 - \beta$ where β is the error of type II (failing to reject a false null hypothesis) and expresses as

$$p = P(\text{Rejecting } H_0 | H_1 \text{ true}).$$

The closer to 1 the power is, the better the test is at detecting a false null hypothesis. For a given forecast f , we write the hypothesis test as:

$$\begin{cases} H_0 : \mathbb{E}(s(f, X)) = \mathbb{E}(s(f_0, X)), \\ H_1 : \mathbb{E}(s(f, X)) \neq \mathbb{E}(s(f_0, X)) \end{cases} \quad (16)$$

where f_0 and f are respectively the perfect forecast and an imperfect f . We consider the additive Gaussian model (A) for the log-score, where the forecast, X and Y are assumed to be normally distributed with an additive error. The expectation in (16) is computed over a $N = 1000$ verification data-points, being the true state X and the corrupted data Y . The power p of the test is computed over 10000 samples of length N . In Figure 5, the power of the above test is shown for varying mean μ and standard deviation σ of the forecast f in order to demonstrate the ability of the proposed score $s_v(., Y)$ to better discriminate between forecasts than the commonly used score $s(., Y)$. One expects the power to be low at respectively μ_0 and σ_0 , and as high as possible outside these values. We notice that the ideal score s_0 and the proposed score have a similar power for the test (16) suggesting similar discriminating skills for both scores. However, the commonly used in practice score $s(., Y)$ shows severe lack of power as the observational noise increases (from left to right), indicating the necessity to account for the uncertainty associated with the verification data. Both varying mean and standard deviation reveal similar conclusions regarding the ability of the proposed score to improve its discriminative skills over a score evaluated on corrupted evaluation data.

5.2 Distance between scores distributions

In order to further study the impact of imperfect verification data and to take full advantages of the score distributions we compute the Wasserstein distance Muskulus and Verduyn-Lunel (2011); Santambrogio (2015); Robin et al. (2017) between several scores distributions and compare it to the commonly used score average. The R-package transport (Schuhmacher et al., 2020) is used to compute Wasserstein distances. Figure 6 shows the mean of the log-score minus its minimum ($\mathbb{E}(s_0(f_0, X))$) and the relative difference between the ideal mean log-score and the mean log-score evaluated against imperfect verification data. One can first observe the flatness of the mean log-score around its minimum indicating a lack of discriminative skills of the score mean when comparing several forecasts. Secondly, the discrepancy between the score evaluated against perfect and imperfect verification data indicates the effects of error prone verification data as discussed earlier. Figure 7 shows the Wasserstein distance between the distributions of scores evaluated for a perfect forecast and an imperfect forecast. Three different log-scores are considered the ideal log-score $s_0(., X)$, the log-score used in practice $s_0(., Y)$ and the proposed corrected score $s_v(., Y)$. One can notice that Wasserstein distances exhibit stronger gradients than the mean log-score indicating

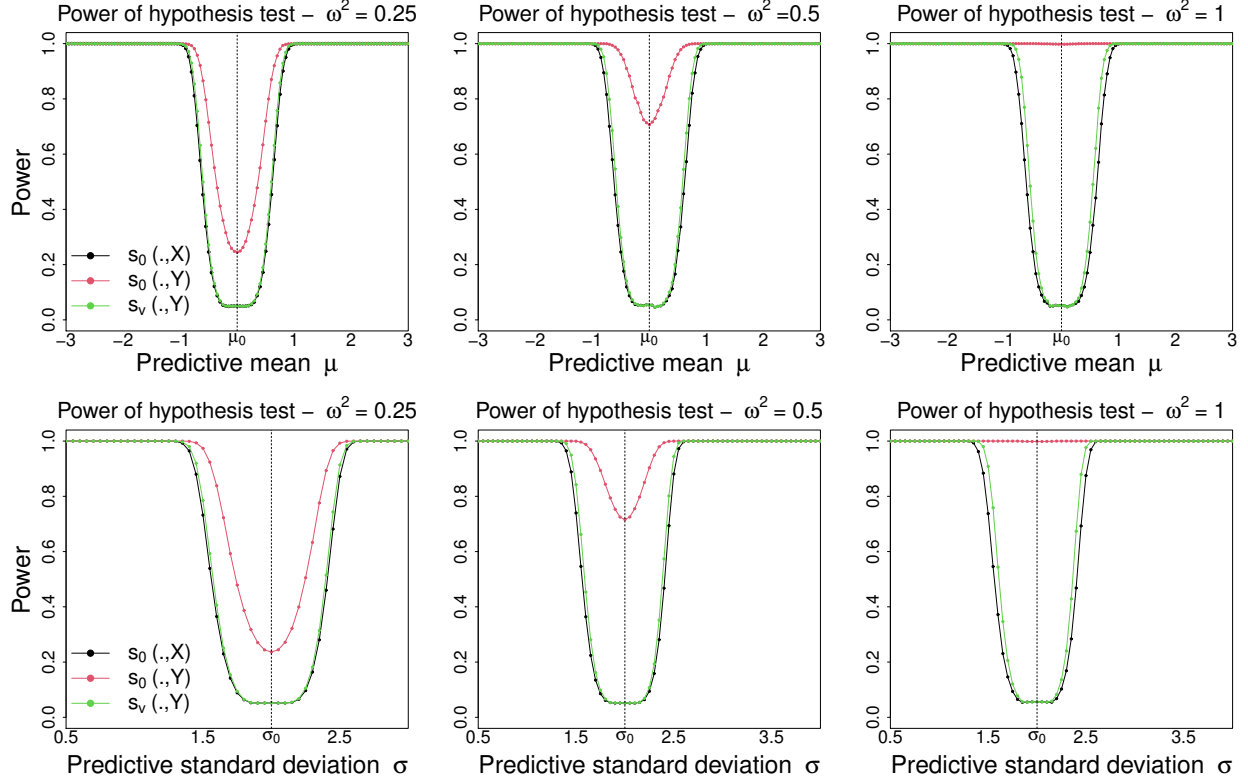


Figure 5: Power of the test (16) against varying predictive mean μ (top) and against varying predictive standard deviation σ (bottom) of the forecast f for different observational noise levels $\omega^2 = 0.25$ (left), $\omega^2 = 0.5$ (central) and $\omega^2 = 1$ (right). In the simulations, the true state X is distributed as $\mathcal{N}(\mu_0 = 0, \sigma_0^2 = 4)$ and Y is distributed as $\mathcal{N}(0, \sigma_0^2 + \omega^2)$. The power expected to be low around μ_0 (resp. σ_0) and as large as possible elsewhere.

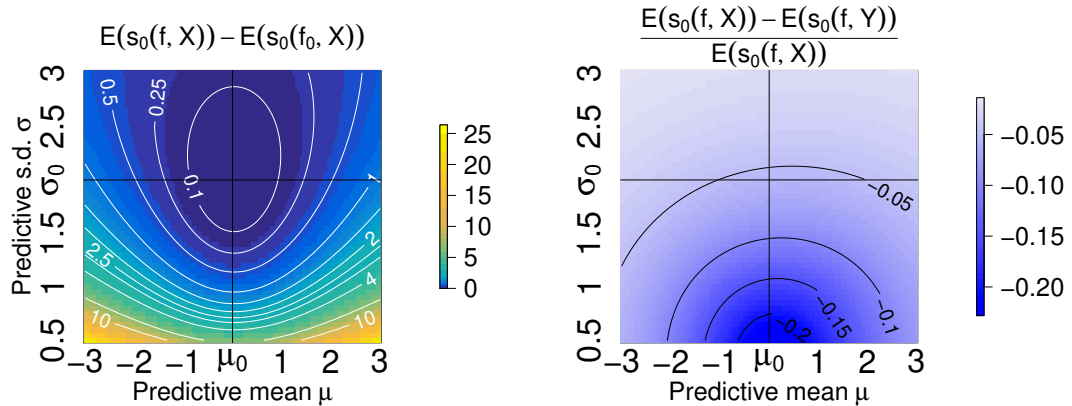


Figure 6: Left: Mean log-score for an imperfect forecast f minus the mean log-score of the ideal forecast f_0 when evaluated against perfect data X , the imperfect forecast $f \sim \mathcal{N}(\mu, \sigma)$ has varying mean μ (x-axis) and varying standard deviation σ (y-axis). Right: Relative difference between $\mathbb{E}(s_0(f, X))$ and $\mathbb{E}(s_0(f, Y))$.

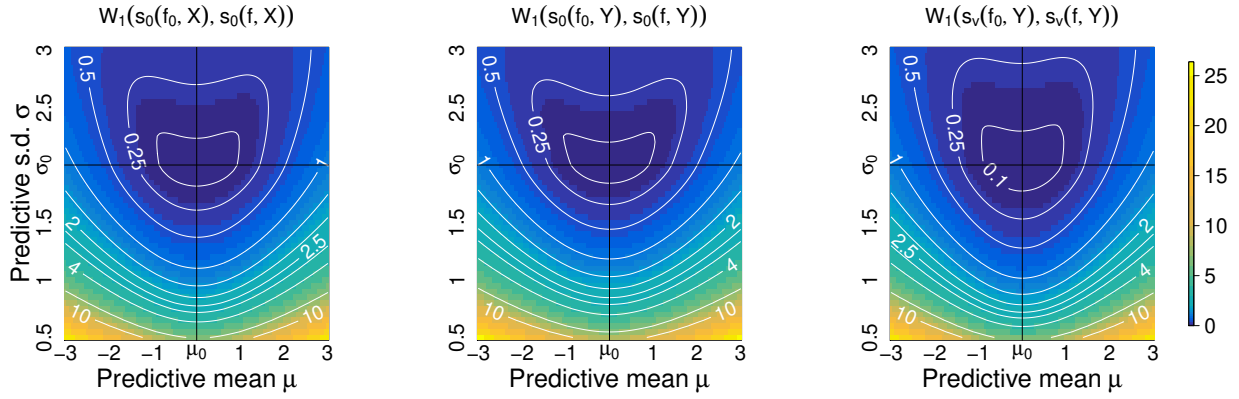


Figure 7: Bottom row: Wasserstein distance $W_1(s_0(f_0, \cdot), s_0(f, \cdot))$ between log-scores s_0 distributions evaluated at the ideal forecast f_0 and the forecast f with varying predictive mean μ (x-axis) and varying predictive standard deviation σ (y-axis). From left to right, log-scores are evaluated against the hidden true state X via $s_0(f, X)$, against Y tainted by observational noise of level $\omega^2 = 1$ via $s_0(f, Y)$ and through the corrected log-score version $s_v(f, Y)$. The verification data X and ideal forecast f_0 are distributed according to $f_0 \sim \mathcal{N}(0, 4)$.

that considering the entire score distribution have the potential to improve the discriminative skills of scoring procedures. In particular, the surfaces delimited by a given contour level are smaller for the proposed score than for the other scores. Finally, when considering Wasserstein distances associated with the score evaluated on imperfect verification data the minimum of the distances is close to the ‘true’ minimum. This indicates some robustness of the Wasserstein distance between the score distributions when errors are present in the verification data. Similar results are obtained for the CRPS and not reported here. As stated earlier, developing metrics to express the discriminative skills of a score is beyond the extent of this work.

5.3 Application to wind speed prediction

As discussed in the motivating example of Section 1, we consider surface wind speed data from the previous work (Bessac et al., 2018) and associated probabilistic distributions. The data are Box-Cox-transformed in this study to approximate normal distributions. In the following, we evaluate the probability distribution of the NWP model outputs depicted in Figure 2. In Bessac et al. (2018), the target distribution was the fitted distribution of the observations; however in the validation step of the predictive probabilistic model, the observations shown in Figure 2 were used without accounting of their potential uncertainty and error. This leads to a discrepancy between the target variable X_{ref} and the verification data that we denote as Y_{obs} . The marginal distributions of X_{ref} and NWP model are extracted from the joint distribution of observations and NWP model outputs proposed in (Bessac et al., 2018). From Pinson and Hagedorn (2012), a reasonable model for unbiased measurement error in wind speed is $\epsilon_{obs} \sim \mathcal{N}(0, 0.25)$. Subsequently to Section 3, we proposed the following additive framework to account for the observational noise in the scoring framework:

$$\begin{cases} X_{ref} \sim \mathcal{N}(\mu_0, \sigma_0^2), \mu_0 \text{ and } \sigma_0 \text{ retrieved from joint model} \\ Y_{obs} = X_{ref} + \epsilon_{obs}, \text{ with } \epsilon_{obs} \sim \mathcal{N}(0, 0.25), \end{cases}$$

	Mean Score	NWP Prediction
Log-score	Ideal score $\mathbb{E}(s_0(f, X))$	1.76
	$\mathbb{E}(s_0(f, Y))$	1.97 (1.52)
	$\mathbb{E}(s_v(f, Y))$	1.81 (1.15)
CRPS	Ideal score $\mathbb{E}(c_0(f, X))$	0.73
	$\mathbb{E}(c_0(f, Y))$	0.82 (0.67)
	$\mathbb{E}(c_v(f, Y))$	0.73 (0.48)

Table 1: Average scores (log-score and CRPS) computed for the predictive distribution of NWP model 1. The mean ideal score $\mathbb{E}(s_0(f, X))$, the averaged score computed in practice against the measurements $\mathbb{E}(s_0(f, Y))$, and the proposed score $\mathbb{E}(s_v(f, X))$ embedding the error in the verification data are computed.

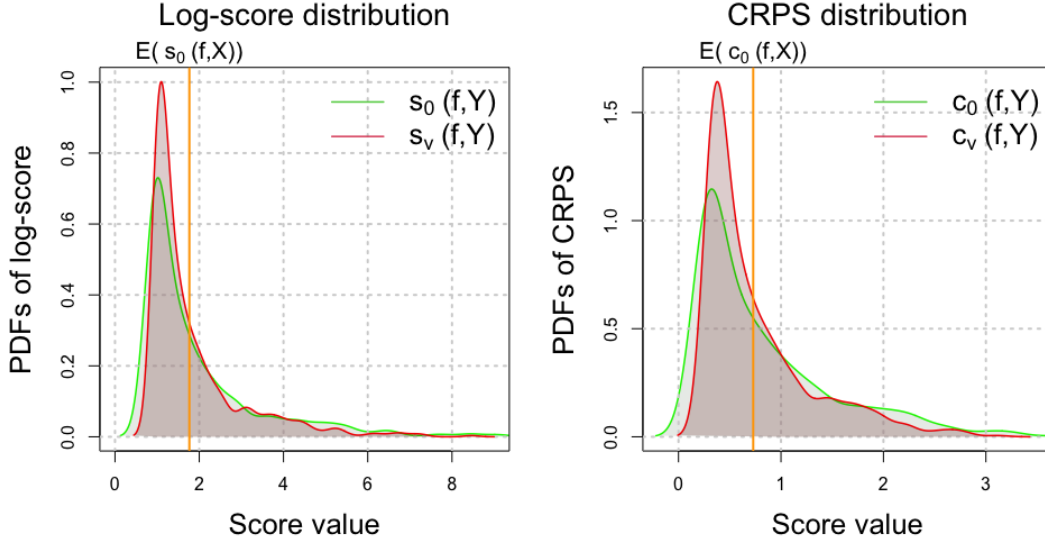


Figure 8: Empirical distribution of uncorrected (green) and corrected scores (red) for the log-score (left) and CRPS (right) for the probabilistic distribution NWP model 1 evaluated against observations tainted with uncertainty. The ideal mean score value is illustrated by the orange vertical line.

where $\mu_0 = 2.55$ and $\sigma_0 = 1.23$ from the fitted distribution. In Table 1, log-scores and CRPS are computed in the additive Gaussian case with previously given formula in Section 3. Table 1 shows a significant decrease of the variance when the proposed score is used compared the commonly used in practice score that does not account for measurement error. One can notice that the variance of the scores used in practice are considerably high limiting the reliability of these computed scores for decision-making purposes. Additionally, the new mean scores are closer to the ideal mean log-score and CRPS, showing the benefit of accounting for observational errors in the scoring framework. Figure 8 shows the pdf of the scores considered in Table 1, the skewness and the large dispersion in the upper tail illustrates with wind speed data cases where the mean is potentially a not informative summary statistics of the whole distribution. The non-corrected version of the score has a large variance, raising the concern of reliability on scores when computed on error-prone data.

6 Discussion

We have quantified, in terms of variance and even distribution, the need to account for the error associated with the verification data when evaluating probabilistic forecasts with scores. An additive framework and a multiplicative framework have been studied in detail to account for the error associated with verification data. Both setups involve a probabilistic model for the accounted errors and a probabilistic description of the underlying non-observed physical process. Although we look only at idealized cases where the parameters of the involved distributions are known, this approach enables us to understand the importance of accounting for the error associated with the verification data. Moreover, the study raises the important point of investigating the distribution of scores when the verification data is considered to be a random variable. Indeed, investigating the means of scores may not provide sufficient information to compare between score discriminative capabilities. This topic has been extensively discussed by Bolin and Wallin (2019) in the context of varying predictability that generates non-homogeneity in the score values that is poorly represented by an average. One could choose to take into account the uncertainty associated with the inference of distribution parameters and compute different statistics of the distribution rather than the mean. In this case, a Bayesian setup could elegantly integrate the different hierarchies of knowledge and a priori information.

Acknowledgments

We thank Aurélien Ribes for his helpful comments and discussions. We also thank the Office of Science and Technology of the Embassy of France in the United States, Washington, DC, for supporting our collaboration through the initiative Make Our Planet Great Again. The effort of Julie Bessac is based in part on work supported by the U.S. Department of Energy, Office of Science, Office of Advanced Scientific Computing Research (ASCR) under Contract DE-AC02-06CH11347. Part of P. Naveau's work was supported by the European DAMOCLES-COST-ACTION on compound events, and he also benefited from French national programs, in particular FRAISE-LEFE/INSU, MELODY-ANR, ANR-11-IDEX-0004 -17-EURE-0006 and ANR T-REX AAP CE40.

7 Appendix

Proof of Equation (2):

For any random variable, say U , its mean can be written conditionally to the random variable y in the following way:

$$\mathbb{E}[U] = \mathbb{E}[\mathbb{E}[U|Y = y]].$$

In our case, the variable $U = s_o(f, X)$ and $s_v(f, y) = \mathbb{E}[U|Y = y]$. This gives $\mathbb{E}[s_v(f, Y)] = \mathbb{E}[s_o(f, X)]$. To show inequality (2), we use the classical variance decomposition

$$\mathbb{V}[U] = \mathbb{V}[\mathbb{E}[U|Y = y]] + \mathbb{E}[\mathbb{V}[U|Y = y]].$$

With our notations, we have

$$\begin{aligned}\mathbb{V}[s_o(f, X)] &= \mathbb{V}[\mathbb{E}[s_o(f, X)|Y = y]] + \mathbb{E}[\mathbb{V}[s_o(f, X)|Y = y]], \\ &= \mathbb{V}[s_v(f, Y)] + \text{a non-negative term.}\end{aligned}$$

This leads to

$$\mathbb{V}[s_o(f, X)] \geq \mathbb{V}[s_v(f, Y)].$$

□

Proof of Equation (5):

To express the score proposed in (1), one needs to derive the conditional distribution $[X|Y = y]$ from Model (A). More precisely, the Gaussian conditional distribution of X given $Y = y$ is equal to

$$[X|Y = y] \sim \mathcal{N}\left(\bar{y}, \frac{\omega^2 \sigma_0^2}{\sigma_0^2 + \omega^2}\right),$$

where \bar{y} is a weighted sum that updates the prior information about $X \sim \mathcal{N}(\mu_0, \sigma_0^2)$ with the observation $Y \sim \mathcal{N}(\mu_0, \sigma_0^2 + \omega^2)$,

$$\bar{Y} = \frac{\omega^2}{\sigma_0^2 + \omega^2} \mu_0 + \frac{\sigma_0^2}{\sigma_0^2 + \omega^2} Y \sim \mathcal{N}\left(\mu_0, \sigma_0^2 \times \frac{\sigma_0^2}{\sigma_0^2 + \omega^2}\right).$$

Combining this information with Equations (1) and (3) leads to

$$\begin{aligned}s_v(f, y) &= \log \sigma + \frac{1}{2\sigma^2} \left\{ \mathbb{E}[(X - \mu)^2|Y = y] \right\} + \frac{1}{2} \log 2\pi, \\ &= \log \sigma + \frac{1}{2\sigma^2} \left\{ \mathbb{V}[X|Y = y] + (\mathbb{E}[X|Y = y] - \mu)^2 \right\} + \frac{1}{2} \log 2\pi, \\ &= \log \sigma + \frac{1}{2\sigma^2} \left\{ \frac{\omega^2 \sigma_0^2}{\sigma_0^2 + \omega^2} + \left(\frac{\omega^2}{\sigma_0^2 + \omega^2} \mu_0 + \frac{\sigma_0^2}{\sigma_0^2 + \omega^2} y - \mu \right)^2 \right\} + \frac{1}{2} \log 2\pi.\end{aligned}$$

By construction, we have

$$\mathbb{E}_Y(s_v(f, Y)) = \mathbb{E}_{\bar{Y}}(s_v(f, \bar{Y})) = \mathbb{E}_X(s_o(f, X)).$$

This means that, to obtain the right score value, we can first compute \bar{Y} as the best estimator of the unobserved X and then use it into in the corrected score $s_v(f, \bar{Y})$. □

Proof of Equation (8):

To compute the corrected CRPS, one needs to calculate the conditional expectation of $c_0(f, X)$ under the distribution of $[X|Y = y]$. We first compute the expectation $E(c_0(f, X))$ and then substitute X by \bar{Y} and its distribution with mean $a = \bar{y}$ and standard deviation $b = \sqrt{\frac{\omega^2 \sigma_0^2}{\sigma_0^2 + \omega^2}}$. From Equation (7) we obtain

$$\mathbb{E}(c_0(f, X)) = \mathbb{E}(X) + 2\sigma \left[\mathbb{E}\left(\phi\left(\frac{X - \mu}{\sigma}\right)\right) - \mathbb{E}\left(\frac{X - \mu}{\sigma} \Phi_0\left(\frac{X - \mu}{\sigma}\right)\right) \right] - \left[\mu + \frac{\sigma}{\sqrt{\pi}} \right].$$

If X follows a normal distribution with mean a and variance b^2 , that is, $X = a + bZ$ with Z a standard random variable, then we can define the continuous function $h(z) = \bar{\Phi}\left(\frac{a+bz-\mu}{\sigma}\right)$, with $h'(z) = -\frac{b}{\sigma}\phi\left(\frac{a+bz-\mu}{\sigma}\right)$. Then, we apply Stein's lemma (Stein, 1981), which states $\mathbb{E}[h'(Z)] = \mathbb{E}[Zh(Z)]$, because Z is a standard random variable. It follows with the notations $t = \frac{b^2}{2\sigma^2}$ and $\lambda = \frac{a-\mu}{\sigma}$ that

$$\begin{aligned}\mathbb{E}\left[\frac{X-\mu}{\sigma}\bar{\Phi}\left(\frac{X-\mu}{\sigma}\right)\right] &= \lambda\mathbb{E}\left[\bar{\Phi}\left(\lambda + \frac{b}{\sigma}Z\right)\right] + \frac{b}{\sigma}\mathbb{E}[Zh(Z)], \\ &= \lambda\mathbb{E}\left(\mathbb{P}\left[Z' > \left(\lambda + \frac{b}{\sigma}Z\right)\right]\right) + \frac{b}{\sigma}\mathbb{E}[h'(Z)], \\ &\quad \text{where } Z' \text{ has a standard normal distribution} \\ &= \lambda\mathbb{E}\left(\mathbb{P}\left[Z' - \frac{b}{\sigma}Z > \lambda\right]\right) - \frac{b^2}{\sigma^2}\mathbb{E}\left[\phi\left(\frac{a+bZ-\mu}{\sigma}\right)\right],\end{aligned}$$

with

$$\begin{aligned}\lambda\mathbb{P}\left[Z' - \frac{b}{\sigma}Z > \lambda\right] &= \lambda\bar{\Phi}\left[\frac{\lambda}{\sqrt{1+b^2/\sigma^2}}\right] = \lambda\bar{\Phi}\left[\frac{a-\mu}{\sqrt{\sigma^2+b^2}}\right] \\ &= \frac{a-\mu}{\sigma}\bar{\Phi}\left[\frac{a-\mu}{\sqrt{\sigma^2+b^2}}\right].\end{aligned}$$

Then

$$\mathbb{E}\left[\frac{X-\mu}{\sigma}\bar{\Phi}\left(\frac{X-\mu}{\sigma}\right)\right] = \frac{a-\mu}{\sigma}\bar{\Phi}\left[\frac{a-\mu}{\sqrt{\sigma^2+b^2}}\right] - \frac{b^2}{\sigma^2}\mathbb{E}\left[\phi\left(\frac{a+bZ-\mu}{\sigma}\right)\right],$$

and

$$\begin{aligned}\mathbb{E}\left[\phi\left(\frac{a+bZ-\mu}{\sigma}\right)\right] &= \frac{1}{\sqrt{2\pi}}\mathbb{E}\left(\exp\left(-\frac{1}{2}\left(\frac{a+bZ-\mu}{\sigma}\right)^2\right)\right) \\ &= \frac{1}{\sqrt{2\pi}}\mathbb{E}\left(\exp\left(-\frac{b^2}{2\sigma^2}\left(Z + \frac{a-\mu}{b}\right)^2\right)\right)\end{aligned}$$

$\left(Z + \frac{a-\mu}{b}\right)^2$ is a noncentered chi-square distribution with one degree of freedom and a noncentral parameter $\left(\frac{a-\mu}{b}\right)^2$ with known moment generating function

$$G\left(t; k=1, \lambda = \left(\frac{a-\mu}{b}\right)^2\right) = \frac{\exp(\frac{\lambda t}{1-2t})}{(1-2t)^{k/2}}.$$

It follows that

$$\begin{aligned}\mathbb{E}\left[\phi\left(\frac{a+bZ-\mu}{\sigma}\right)\right] &= \frac{1}{\sqrt{2\pi}}G\left(t = \frac{-b^2}{2\sigma^2}; k=1, \lambda = \left(\frac{a-\mu}{b}\right)^2\right) \\ &= \frac{1}{\sqrt{2\pi}}\frac{\exp\left(\frac{-\frac{(a-\mu)^2}{b^2}\frac{b^2}{2\sigma^2}}{1+\frac{b^2}{\sigma^2}}\right)}{\sqrt{(1+\frac{b^2}{\sigma^2})}} \\ &= \frac{\sigma}{\sqrt{2\pi}\sqrt{\sigma^2+b^2}}\exp\left(\frac{-(a-\mu)^2}{2(\sigma^2+b^2)}\right).\end{aligned}$$

We obtain

$$\begin{aligned}
E(c_0(f, X)) &= E(X) + 2\sigma \left[\left(1 + \frac{b^2}{\sigma^2}\right) E\left(\phi\left(\frac{X - \mu}{\sigma}\right)\right) - \frac{a - \mu}{\sigma} \bar{\Phi}\left[\frac{a - \mu}{\sqrt{\sigma^2 + b^2}}\right] \right] - \left(\mu + \frac{\sigma}{\sqrt{\pi}}\right) \\
&= E(X) + 2\sigma \left[\left(1 + \frac{b^2}{\sigma^2}\right) \frac{\sigma}{\sqrt{2\pi(\sigma^2 + b^2)}} \exp\left(\frac{-(a - \mu)^2}{2(\sigma^2 + b^2)}\right) - \frac{a - \mu}{\sigma} \bar{\Phi}\left[\frac{a - \mu}{\sqrt{\sigma^2 + b^2}}\right] \right] \\
&\quad - \left(\mu + \frac{\sigma}{\sqrt{\pi}}\right) \\
&= E(X) + 2 \left[\frac{\sqrt{\sigma^2 + b^2}}{\sqrt{2\pi}} \exp\left(\frac{-(a - \mu)^2}{2(\sigma^2 + b^2)}\right) - (a - \mu) \bar{\Phi}\left[\frac{a - \mu}{\sqrt{\sigma^2 + b^2}}\right] \right] \\
&\quad - \left(\mu + \frac{\sigma}{\sqrt{\pi}}\right).
\end{aligned}$$

The expression of (8) is obtained by substituting X by \bar{Y} and its Gaussian distribution with mean $a = \bar{y}$ and standard deviation $b = \sqrt{\frac{\omega^2 \sigma_0^2}{\sigma_0^2 + \omega^2}}$ in the expression (6). This gives

$$\begin{aligned}
c_v(f, \bar{y}) &= E(c_0(f, X) | Y = y) \\
&= \bar{y} - \left(\mu + \frac{\sigma}{\sqrt{\pi}}\right) \\
&\quad + 2 \left(\frac{\sqrt{\sigma^2 + \frac{\sigma_0^2 \omega^2}{\sigma_0^2 + \omega^2}}}{\sqrt{2\pi}} \exp\left(-\frac{(\bar{y} - \mu)^2}{2(\sigma^2 + \frac{\omega^2 \sigma_0^2}{\sigma_0^2 + \omega^2})}\right) - (\bar{y} - \mu) \Phi\left(\frac{\bar{y} - \mu}{\sqrt{\sigma^2 + \frac{\omega^2 \sigma_0^2}{\sigma_0^2 + \omega^2}}}\right) \right).
\end{aligned}$$

□

Proof of Equation (9):

For Model (A), both random variables Y and $\bar{Y} = \frac{\omega^2}{\sigma_0^2 + \omega^2} \mu_0 + \frac{\sigma_0^2}{\sigma_0^2 + \omega^2} Y$ are normally distributed with the same mean μ_0 but different variances, $\sigma_0^2 + \omega^2$ and $\left(\frac{\sigma_0^2}{\sigma_0^2 + \omega^2}\right)^2 (\sigma_0^2 + \omega^2)$, respectively. Since a chi-square distribution can be defined as the square of a Gaussian random variable, it follows from Eqn. (5) that

$$s_0(f, Y) \stackrel{d}{=} a_0 + b_0 \chi_0^2 \text{ and } s_v(f, Y) \stackrel{d}{=} a_v + b_v \chi_v^2,$$

where $\stackrel{d}{=}$ means equality in distribution and

$$a_0 = \log \sigma + \frac{1}{2} \log 2\pi \quad \text{and} \quad b_0 = \frac{\sigma_0^2 + \omega^2}{2\sigma^2},$$

$$a_v = \log \sigma + \frac{1}{2\sigma^2} \frac{\omega^2 \sigma_0^2}{\sigma_0^2 + \omega^2} + \frac{1}{2} \log 2\pi \quad \text{and} \quad b_v = \frac{\sigma_0^2 + \omega^2}{2\sigma^2} \left(\frac{\sigma_0^2}{\sigma_0^2 + \omega^2}\right)^2,$$

with χ_0^2 and χ_v^2 representing noncentral chi-squared random variable with one degree of freedom and noncentrality parameter

$$\lambda_0 = \frac{(\mu_0 - \mu)^2}{\sigma_0^2 + \omega^2} \text{ and } \lambda_v = \frac{(\mu_0 - \mu)^2}{\sigma_0^2 + \omega^2} \left(\frac{\sigma_0^2 + \omega^2}{\sigma_0^2}\right)^2.$$

□

Proof of Equation (13):

In Model (B), the basic conjugate prior properties of such gamma and inverse gamma distributions allow us to say that $[X|Y = y]$ now follows a gamma distribution with parameters $\alpha_0 + a$ and $\beta_0 + b/y$

$$f_{X|Y=y}(x|y) = \frac{(\beta_0 + b/y)^{\alpha_0+a}}{\Gamma(\alpha_0 + a)} x^{\alpha_0+a-1} \exp(-x(\beta_0 + b/y)), \text{ for } x > 0.$$

It follows that the proposed corrected score is

$$\begin{aligned} s_v(f, y) &= \mathbb{E}[s_o(f, X)|Y = y] \\ &= (1 - \alpha)\mathbb{E}[\log(X)|Y = y] + \beta\mathbb{E}[X|Y = y] - \alpha \log \beta + \log \Gamma(\alpha), \\ &= (1 - \alpha) \left(\psi(\alpha_0 + a) - \log \left(\beta_0 + \frac{b}{y} \right) \right) + \beta \frac{\alpha_0 + a}{\beta_0 + \frac{b}{y}} - \alpha \log \beta + \log \Gamma(\alpha). \end{aligned}$$

Indeed $\mathbb{E}[X|Y = y] = \frac{\alpha_0+a}{\beta_0+\frac{b}{y}}$ and $\mathbb{E}[\log(X)|Y = y] = \psi(\alpha_0 + a) - \log \left(\beta_0 + \frac{b}{y} \right)$ where $\psi(x)$ represents the digamma function defined as the logarithmic derivative of the gamma function, namely, $\psi(x) = d \log \Gamma(x)/dx$. \square

Proof of Equation (15):

From Equation (14) we obtain

$$c_v(f, y) = \mathbb{E}[X|Y = y] - \left[\frac{\alpha}{\beta} + \frac{1}{\beta B(.5, \alpha)} \right] + 2 \left[\mathbb{E} \left[\frac{X}{\beta} f(X) | Y = y \right] + \mathbb{E} \left[\left(\frac{\alpha}{\beta} - X \right) \bar{F}(X) | Y = y \right] \right].$$

Since the conditional distribution of $[X|Y = y]$ is known:

$$\begin{aligned} \mathbb{E} \left[\frac{X}{\beta} f(X) | Y = y \right] &= \frac{1}{\beta} \int_0^{+\infty} x f(x) \frac{(\beta_0 + b/y)^{\alpha_0+a}}{\Gamma(\alpha_0 + a)} x^{\alpha_0+a-1} \exp(-x(\beta_0 + b/y)) dx \\ &= \frac{\beta^{\alpha-1} (\beta_0 + b/y)^{\alpha_0+a}}{\Gamma(\alpha) \Gamma(\alpha_0 + a)} \int_0^{+\infty} x^{\alpha+\alpha_0+a-1} \exp(-(\beta + \beta_0 + b/y)x) dx \\ &= \frac{\beta^{\alpha-1} (\beta_0 + b/y)^{\alpha_0+a}}{\Gamma(\alpha) \Gamma(\alpha_0 + a)} \frac{1}{(\beta + \beta_0 + b/y)^{\alpha+\alpha_0+a}} \int_0^{+\infty} u^{\alpha+\alpha_0+a-1} \exp(-u) du \\ &= \frac{\beta^{\alpha-1} (\beta_0 + b/y)^{\alpha_0+a}}{\Gamma(\alpha) \Gamma(\alpha_0 + a)} \frac{\Gamma(\alpha + \alpha_0 + a)}{(\beta + \beta_0 + b/y)^{\alpha+\alpha_0+a}} \\ &= \frac{\beta^{\alpha-1} (\beta_0 + b/y)^{\alpha_0+a}}{B(\alpha, \alpha_0 + a) (\beta + \beta_0 + b/y)^{\alpha+\alpha_0+a}}, \end{aligned}$$

and the last term

$$\begin{aligned} \mathbb{E} \left(\left(\frac{\alpha}{\beta} - X \right) \bar{F}(X) | Y = y \right) &= \frac{(\beta_0 + b/y)^{\alpha_0+a}}{\Gamma(\alpha_0 + a)} \int_0^{+\infty} \left(\frac{\alpha}{\beta} - x \right) \left(\int_x^{+\infty} \frac{\beta^\alpha}{\Gamma(\alpha)} u^{\alpha-1} \exp(-\beta u) du \right) \\ &\quad \times x^{\alpha_0+a-1} \exp(-(\beta_0 + b/y)x) dx \\ &\quad \text{with } \int_x^{+\infty} \frac{\beta^\alpha}{\Gamma(\alpha)} u^{\alpha-1} \exp(-\beta u) du = \frac{1}{\Gamma(\alpha)} \int_{\beta x}^{+\infty} v^{\alpha-1} \exp(-v) dv \\ &= \frac{(\beta_0 + b/y)^{\alpha_0+a}}{\Gamma(\alpha) \Gamma(\alpha_0 + a)} \int_0^{+\infty} \left(\frac{\alpha}{\beta} - x \right) \Gamma(\alpha, \beta x) x^{\alpha_0+a-1} \exp(-(\beta_0 + b/y)x) dx, \end{aligned}$$

where $\Gamma(\alpha, \beta x) = \int_{\beta x}^{+\infty} v^{\alpha-1} \exp(-v) dv$ is the upper incomplete gamma function. The entire expression of the corrected CRPS expresses as

$$\begin{aligned} c_v(f, y) &= \left[\frac{\alpha}{\beta} - \frac{1}{\beta B(.5, \alpha)} \right] - \frac{\alpha_0 + a}{\beta_0 + \frac{b}{y}} + 2 \frac{\beta^{\alpha-1} (\beta_0 + b/y)^{\alpha_0+a}}{B(\alpha, \alpha_0 + a) (\beta + \beta_0 + b/y)^{\alpha+\alpha_0+a}} \\ &+ 2 \frac{(\beta_0 + b/y)^{\alpha_0+a}}{\Gamma(\alpha) \Gamma(\alpha_0 + a)} \int_0^{+\infty} \left(\frac{\alpha}{\beta} - x \right) \Gamma(\alpha, \beta x) x^{\alpha_0+a-1} \exp(-(\beta_0 + b/y)x) dx. \end{aligned}$$

□

References

- Anderson, J. L. (1996). A method for producing and evaluating probabilistic forecasts from ensemble model integrations. *Journal of Climate*, 9(7):1518–1530.
- Bessac, J., Constantinescu, E., and Anitescu, M. (2018). Stochastic simulation of predictive space-time scenarios of wind speed using observations and physical model outputs. *The Annals of Applied Statistics*, 12(1):432–458.
- Bolin, D. and Wallin, J. (2019). Scale invariant proper scoring rules scale dependence: Why the average crps often is inappropriate for ranking probabilistic forecasts. *arXiv preprint arXiv:1912.05642*.
- Bowler, N. E. (2008). Accounting for the effect of observation errors on verification of mogreps. *Meteorological Applications*, 15(1):199–205.
- Bröcker, J. and Ben Bouallègue, Z. (2020). Stratified rank histograms for ensemble forecast verification under serial dependence. *Quarterly Journal of the Royal Meteorological Society*, 146(729):1976–1990.
- Candille, G. and Talagrand, O. (2008). Retracted and replaced: Impact of observational error on the validation of ensemble prediction systems. *Quarterly Journal of the Royal Meteorological Society*, 134(631):509–521.
- Ciach, G. J. and Krajewski, W. F. (1999). On the estimation of radar rainfall error variance. *Advances in Water Resources*, 22(6):585–595.
- Daley, R. (1993). Estimating observation error statistics for atmospheric data assimilation. *Annales Geophysicae*, 11:634–647.
- Diebold, F. X. and Mariano, R. S. (2002). Comparing predictive accuracy. *Journal of Business & economic statistics*, 20(1):134–144.
- Dirkson, A., Merryfield, W. J., and Monahan, A. H. (2019). Calibrated probabilistic forecasts of arctic sea ice concentration. *Journal of Climate*, 32(4):1251–1271.
- Ferro, C. A. T. (2017). Measuring forecast performance in the presence of observation error. *Quarterly Journal of the Royal Meteorological Society*, 143(708):2665–2676.

- Gneiting, T., Balabdaoui, F., and Raftery, A. E. (2007). Probabilistic forecasts, calibration and sharpness. *Journal of the Royal Statistical Society: Series B (Statistical Methodology)*, 69(2):243–268.
- Gneiting, T. and Raftery, A. E. (2007). Strictly proper scoring rules, prediction, and estimation. *Journal of the American Statistical Association*, 102(477):359–378.
- Gneiting, T., Raftery, A. E., Westveld III, A. H., and Goldman, T. (2005). Calibrated probabilistic forecasting using ensemble model output statistics and minimum CRPS estimation. *Monthly Weather Review*, 133(5):1098–1118.
- Gorgas, T. and Dorninger, M. (2012). Quantifying verification uncertainty by reference data variation. *Meteorologische Zeitschrift*, 21(3):259–277.
- Hamill, T. M. (2001). Interpretation of rank histograms for verifying ensemble forecasts. *Monthly Weather Review*, 129(3):550–560.
- Hamill, T. M. and Juras, J. (2006). Measuring forecast skill: Is it real skill or is it the varying climatology? *Quarterly Journal of the Royal Meteorological Society*, 132(621C):2905–2923.
- Janjić, T., Bormann, N., Bocquet, M., Carton, J. A., Cohn, S. E., Dance, S. L., Losa, S. N., Nichols, N. K., Potthast, R., Waller, J. A., and Weston, P. (2017). On the representation error in data assimilation. *Quarterly Journal of the Royal Meteorological Society*.
- Jolliffe, I. T. (2007). Uncertainty and inference for verification measures. *Weather and Forecasting*, 22(3):637–650.
- Jolliffe, T. and Stephenson, D. B. (2004). Forecast verification: A practitioner’s guide in atmospheric science. edited by ian wiley, chichester, 2003. xiv+240 pp. isbn 0 471 49759 2. *Weather*, 59(5):132–132.
- Kalman, R. E. (1960). A new approach to linear prediction and filtering problems. *Transactions of the ASME—Journal of Basic Engineering*, pages 35–45.
- Kalman, R. E. and Bucy, R. S. (1961). New results in linear filtering and prediction theory.
- Kleen, O. (2019). Measurement error sensitivity of loss functions for distribution forecasts. *Available at SSRN 3476461*.
- Mittermaier, M. P. and Stephenson, D. B. (2015). Inherent bounds on forecast accuracy due to observation uncertainty caused by temporal sampling. *Monthly Weather Review*, 143(10):4236–4243.
- Murphy, A. H. (1973). A new vector partition of the probability score. *Journal of Applied Meteorology*, 12(4):595–600.
- Murphy, A. H. and Winkler, R. L. (1987). A general framework for forecast verification. *Monthly Weather Review*, 115(7):1330–1338.
- Muskulus, M. and Verduyn-Lunel, S. (2011). Wasserstein distances in the analysis of time series and dynamical systems. *Physica D: Nonlinear Phenomena*, 240(1):45–58.

- Pappenberger, F., Ghelli, A., Buizza, R., and Bodis, K. (2009). The skill of probabilistic precipitation forecasts under observational uncertainties within the generalized likelihood uncertainty estimation framework for hydrological applications. *Journal of Hydrometeorology*, 10(3):807–819.
- Pinson, P. and Hagedorn, R. (2012). Verification of the ecmwf ensemble forecasts of wind speed against analyses and observations. *Meteorological Applications*, 19(4):484–500.
- Robin, Y., Yiou, P., and Naveau, P. (2017). Detecting changes in forced climate attractors with Wasserstein distance. *Nonlinear Processes in Geophysics*, 24(3):393–405.
- Saetra, O., Hersbach, H., Bidlot, J.-R., and Richardson, D. S. (2004). Effects of observation errors on the statistics for ensemble spread and reliability. *Monthly weather review*, 132(6):1487–1501.
- Santambrogio, F. (2015). Optimal transport for applied mathematicians. *Birkhäuser, NY*, 55(58-63):94.
- Scheuerer, M. and Möller, D. (2015). Probabilistic wind speed forecasting on a grid based on ensemble model output statistics. *The Annals of Applied Statistics*, 9(3):1328–1349.
- Schuhmacher, D., Bähre, B., Gottschlich, C., Hartmann, V., Heinemann, F., Schmitzer, B., Schrieber, J., and Wilm, T. (2020). *transport: Computation of Optimal Transport Plans and Wasserstein Distances*. R package version 0.12-2.
- Skamarock, W., Klemp, J., Dudhia, J., Gill, D., Barker, D., Duda, M., Huang, X.-Y., Wang, W., and Powers, J. (2008). A description of the Advanced Research WRF version 3. Technical Report Tech Notes-475+ STR, NCAR.
- Stein, C. M. (1981). Estimation of the mean of a multivariate normal distribution. *The Annals of Statistics*, pages 1135–1151.
- Taillardat, M., Mestre, O., Zamo, M., and Naveau, P. (2016). Calibrated ensemble forecasts using quantile regression forests and ensemble model output statistics. *Monthly Weather Review*, 144(6):2375–2393.
- Waller, J. A., Dance, S. L., Lawless, A. S., and Nichols, N. K. (2014). Estimating correlated observation error statistics using an ensemble transform kalman filter. *Tellus A: Dynamic Meteorology and Oceanography*, 66(1):23294.
- Weijs, S. V. and Van De Giesen, N. (2011). Accounting for observational uncertainty in forecast verification: an information-theoretical view on forecasts, observations, and truth. *Monthly Weather Review*, 139(7):2156–2162.
- Weijs, S. V., Van Nooijen, R., and Van De Giesen, N. (2010). Kullback–Leibler divergence as a forecast skill score with classic reliability–resolution–uncertainty decomposition. *Monthly Weather Review*, 138(9):3387–3399.
- Wilks, D. S. (2010). Sampling distributions of the brier score and brier skill score under serial dependence. *Quarterly Journal of the Royal Meteorological Society*, 136(653):2109–2118.

Zamo, M. and Naveau, P. (2018). Estimation of the continuous ranked probability score with limited information and applications to ensemble weather forecasts. *Mathematical Geosciences*, 50(2):209–234.